Inverse Projection of Vector Fields

Paula Ceccon Ribeiro and Hélio Lopes
Departamento de Informtica – Pontifícia Universidade Católica do Rio de Janeiro
Rio de Janeiro, Brazil
Email: {pribeiro,lopes}@inf.puc-rio.br

***Abstract*—Vector fields play an essential role in a large range of scientific applications. They are commonly generated through computer simulations. Such simulations may be a costly process since they usually require an intensive computational time. When researchers want to quantify the uncertainty in such kind of applications, usually an ensemble of vector fields realizations are generated, making the process much more expensive. The main contribution of this paper is to present a new method, based on the inverse projection technique, to quickly and consistently generate 2D vector fields similar to the ones in the ensemble, which after an evaluation of a specialist could enlarge the ensemble in order to better represent the uncertainty. Through the Helmholtz-Hodge Decomposition, we obtain the divergence-free, rotational-free and harmonic components of a vector field. With those components and the original ensemble in hand, it is possible to derive new realizations from their projections into a 2-dimensional space. To do so, we propose the use of an inverse projection technique individually in each component projected space. Results are obtained in real-time, through an interactive interface. A set of multi-method wind forecast realizations were used to demonstrate the results obtained with this approach.**

keywords: Vector Fields; Inverse Projection; Shepard Interpolation

I. Introduction

Modeling a physical spatial/temporal phenomenon is a very important task on several decision making applications [1]. To represent *uncertainty* is for sure a relevant step on this task not only because there is an incomplete understanding of the process itself, but also because it is difficult to restrict their physical parameters [2].

The modeling methods of several physical phenomena under uncertainty have two building blocks: a deterministic and a stochastic. On one side, deterministic models come up with physically-based simulated outcomes. On the other side, stochastic models try to provide realizations that somehow cover the uncertainty space and mimic the physics (providing a certain level of realism) [2] as well. The uncertainty space is generally represented by an ensemble of scenarios.

Vector fields are very important in several problems related to *Scientific Computing*. Applications that make use of vector fields include, for example: fluid flow simulation [3], analysis of MRI data for medical prognosis [4] and weather prediction [5], just to cite a few. The deterministic simulation of vector fields in such applications may require expensive numerical computations [3]. When researchers want to quantify the uncertainty in such kind of applications, usually an ensemble of vector field realizations are generated, making the process much more expensive. The main contribution of this paper is to present a new method based on the inverse projection technique to quickly and consistently generate 2D *vector fields* similar to the ones in the ensemble, which after a evaluation of a specialist could enlarge the ensemble in order to better represent the uncertainty.

The *dimensionality reduction*, or *multidimensional projection*, is an approach used to represent a multidimensional data in a low-dimensional space. Its goal consists in providing an overview of similarities between instances of data in a projection space [6], which can then be visually encoded and interpreted. Many algorithms for dimensionality reduction can be found in the literature. Among them, we can cite the well know PCA [7], MDS [8], t-SNE [9] and LAMP [10].

The *inverse projection* works in the opposite way. Given a multidimensional data set $\{X_1, \ldots, X_n\}$, with $X_i \in \mathbb{R}^m$ and its corresponding 2D projection $\{Y_1, \ldots, Y_n\}$, with $Y_i \in \mathbb{R}^k$, where $k << m$, such technique allows the creation of a new realization X in the input space $\mathbb{R}^m$ given a point Y in the projection space $\mathbb{R}^k$.

We propose two strategies to generate new realizations of vector fields from an ensemble by the use of an inverse projection technique. The first one is accomplished based on the original vector field ensemble. The second one is obtained through the combination of the rotational-free, divergence-free and harmonic components derived from the Helmholtz-Hodge Decomposition (HHD) [11] of each element in the original vector field ensemble. This strategy increases the variability of vector fields that can be obtained, enlarging the range of possible outcomes. Moreover, it is also possible to fix some of the original components to be used in the inverse projection step. In that case, the desirable component will be present in the output data.

The proposed approach can be summarized as follows: the HHD is calculated to obtain the divergence-free, rotational-free and harmonic components of a given set of vector fields. Multidimensional projection is then performed on the original data set as well as on each set of the HHD components. After that, for any point p in the projection space, it can be mapped into the original space to generate a new vector field realization by the use of an interpolation method. Amorim et al. [12] applied the RBF interpolation method to perform the inverse projection; here we propose the use of Shepard's interpolation method because it shows to be more robust. As a next step, a specialist could interpret and include a new realization on the ensemble to enlarge the uncertainty representation.

The remainder of this document is organized as follows: Section II presents some previous and related works. Section III briefly describes the Helmholtz-Hodge Decomposition. Section IV presents the concepts of Multidimensional Projection and Inverse Projection, depicting their applicability to synthesize vector fields from an ensemble. Then, Section V describes the proposed approach to generate vector field realizations from a given data set. In the following, Section VI presents the achieved results of the proposed approach. Finally, Section VII describes final remarks and future works.

II. Related Work

Dimensionality reduction has been largely applied to different problems and research areas. For instance, in [13] one can find a proposal of the use of multidimensional projection for image colorization. Through an interactive tool, users can manipulate the projected data to improve clusters and the colorization results. By the time of the study, the authors concluded that their technique outperformed existing techniques in terms of accuracy and flexibility. As another example, we can cite its applicability on the visual analysis of social network. In [14], the authors describe each individual as an array of attributes, projecting them in a low dimensional space. Hence, they are able to visually encode individuals that are highly related to one another. They also conclude that the achieved results present better node distribution when compared to conventional force-based graph drawing. Finally, other applications of dimensionality reduction include sentiment analysis [15], face recognition [16] and email classification [17].

Working together with the dimensionality reduction technique, the inverse projection provides flexible mechanisms to simultaneously visualize and actively explore high-dimensional spaces [12]. [18] presented a visualization-assisted methodology for interacting and transforming data attributes embedded in feature spaces. In their work, the projected data can then be manipulated to create groups of interest. Changes made in the projection space are then mapped back to the feature space so as to modify the distance relationship among a subset of instances. This is then mapped back to the projection space, in a cycling process. This approach was tested with data sets ranging from spam classification to image segmentation. For each data set, the authors noted an increase in their silhouette after few user interactions, which lead to an improvement in the cohesion and separation of these data sets. They also relate an improvement in accuracy of classification methods. [12], on the other hand, depicts an inverse linear affine multidimensional (iLAMP) projection that enables a novel interactive exploration technique for multidimensional data. Firstly, a given data set is projected onto a 2D space, in which the exploration takes place. Then, iLAMP allows the user to create points and regions in the visual space and map them back into high-dimensional instances, based on the distance of the selected point and the projected data. Following this work, Amorim et al. [6] proposed an inverse projection technique based on the Radial Basis Function interpolation (RBF). Opposite to the iLAMP technique, which is local and piece-wise continuous, the proposed technique provides a smooth and global mapping from low to high dimensions. To test this approach, a 3D human-faces data set was used to interactively reconstruct and generate new 3D faces. According to the authors, results demonstrate the simplicity, robustness and efficiency of the proposed approach to create new face models from a structured data set, a task that would typically require the manipulation of hundreds of parameters. As another example, Motta et al. [19] introduce a interactive framework for unsteady fluid flow segmentation and visualization that uses steady and unsteady vector fields segmentation and combines streamlines, multidimensional projection, and machine learning.

The Helmholtz-Hodge Decomposition aims to rewrite a vector field as a sum of three meaningful components: the rotational-free, the divergence-free and the harmonic components. For a survey about this technique, we recommend the paper of Bhatia et al. [20]. This decomposition is particularly useful to extract features and singularities of a flow [4]. It has been used as an important tool in different fields of study, ranging from complex ocean flow [21] to fingerprint images [22]. Recently, an application of the HHD in the uncertainty analysis of 2D vector field ensembles has been proposed [23].

In this paper we apply these techniques to interactively generate vector fields from an ensemble of vector fields.

III. Helmholtz-Hodge Decomposition

The Helmholtz-Hodge Decomposition describes a vector field as the sum of a divergence-free, a rotational-free and a harmonic component [4]. In this work we will deal with vector fields in $\mathbb{R}^2$.

For a smooth vector field $\mathbf{V} : \mathcal{D} \subset \mathbb{R}^2 \to \mathbb{R}^2$ defined on a bounded or unbounded domain $\mathcal{D}$, there is a decomposition satisfying the following property:

$$\mathbf{V} = \nabla g + J(\nabla r) + \mathbf{h},$$

where g and r are *scalar fields*, $\mathbf{h}$ is a *vector field* and J is an operator that rotates a 2D vector counterclockwise by $\pi/2$ ($J(v_1, v_2) = (-v_2, v_1)$). They satisfy the following equations:

- $\nabla \times (\nabla g) = \mathbf{0}$;
- $\nabla \cdot (J(\nabla r)) = 0$;
- $\nabla \times \mathbf{h} = \mathbf{0}$ and $\nabla \cdot \mathbf{h} = 0$.

Given that, from now on we will name ∇g, $J(\nabla r)$ and $\mathbf{h}$, respectively, the *rotational-free component*, the *divergence-free component*, and the *harmonic component* of $\mathbf{V}$. Moreover, g and r are called the *potential* functions of $\mathbf{V}$.

In order to have an unique Helmholtz-Hodge Decomposition, some special boundary conditions have to be applied [20]. However, these boundary conditions lead to some artifacts in the decomposed vector field components. To overcome this problem, in this paper we decided to adopt the Natural Helmholtz-Hodge Decomposion (NHHD) [24] to decompose a vector field in order to obtain the rotational-free, divergence-free and harmonic components. The NHHD aims to compute, on a point-wise basis, an artifact-free HHD on vector fields with open boundaries or unknown boundary conditions.

IV. Inverse projection of 2D Vector Fields

Consider a discrete sampling of a 2-dimensional domain on a Cartesian grid structure $\mathbb{S}_{r,c} = \{\mathbf{x}_{i,j} \in \mathbb{R}^2 : 1 \leq i \leq r, 1 \leq j \leq c\}$. Also, let $\mathcal{V} = \{\mathbf{V}_1, \ldots, \mathbf{V}_n\}$ be a 2D vector field ensemble, i.e., a set of 2D vector fields where each one is defined in $\mathbb{S}_{r,c}$.

In this section we describe how the concepts of Multidimensional Projection and Inverse Projection can be applied to generate new 2D vector fields from an ensemble $\mathcal{V}$.

A. Multidimensional Scaling

Given an integer $k \geq 2$, a collection of n objects $\mathcal{O} = \{o_1, \ldots, o_n\}$ and a similarity function that returns for each pair i, j of objects in $\mathcal{O}$ the value $\delta_{i,j}$, the *Multidimensional Scaling* (MDS) method [25] associates n objects to n points $\{\mathbf{p}_1, \ldots, \mathbf{p}_n\} \in \mathbb{R}^k$ such that $||\mathbf{p}_i - \mathbf{p}_j||$ approximates $\delta_{i,j}$. The MDS method is usually formulated as a minimization problem whose objective function could be, for example, the so called *stress* function:

$$\left(\frac{\sum_{i=1}^{n} \sum_{j=1, j\neq i}^{n} (||\mathbf{p}_i - \mathbf{p}_j|| - \delta_{i,j})^2}{\sum_{i=1}^{n} \sum_{j=1, j\neq i}^{n} \delta_{i,j}^2} \right)^{1/2}$$

The point $\mathbf{p}_i$ corresponds to the projection of the object $o_i \in \mathcal{O}$ in the space $\mathbb{R}^k$. A poor representation of a high-dimensional data in a $\mathbb{R}^k$ space is reflected on a high stress value. In this paper, we fix the value of k as 2 to facilitate user interaction and visualization.

B. Dissimilarity Matrix of 2D vector fields

As described above, to perform a dimensional reduction on a collection of objects $\mathcal{O}$, it is necessary to obtain a similarity measure for each pair of elements in $\mathcal{O}$. Considering that $\mathcal{O}$ is an ensemble of 2D vector fields $\mathcal{V}$, this means that, for each pair of vector fields $\mathbf{V}_i, \mathbf{V}_j \in \mathcal{V}$ it is necessary to define how close they are to each other. To take into account both the magnitude and orientation of a vector field, we propose the following transformation and similarity measure.

Firstly, for a 2D vector field $\mathbf{V}_i \in \mathcal{V}$, with $\mathbf{V}_i = (v_{i_x}, v_{i_y})$ being defined on the grid $\mathbb{S}_{r,c}$, we rewrite v_{i_x} and v_{i_y} as two $r \times c$ arrays. After that, we transform $\mathbf{V}_i$ by the use of a function F into a pair of features $f1, f2$ according to the following formulas:

$$\begin{aligned} f1_i &= \tfrac{\operatorname{atan2}(v_{i_y}, v_{i_x})}{\pi/2} \\ f2_i &= \tfrac{\|(v_{i_x}, v_{i_y})\|}{\max_{j=1\ldots n}\{f2_j\}} \\ F(\mathbf{V_i}) &= (f1_i, f2_i) \end{aligned}$$

Finally, we define the similarity function δ for each pair of vector fields $\mathbf{V}_i$ and $\mathbf{V}_j$ in $\mathcal{V}$ as the *Cosine Similarity* according to this formula:

$$\delta(\mathbf{V}_i, \mathbf{V}_j) = \delta_{i,j} = \frac{F(\mathbf{V}_i) \cdot F(\mathbf{V}_j)}{\|F(\mathbf{V}_i)\| \cdot \|F(\mathbf{V}_j)\|} \tag{1}$$

We propose two strategies to generate new realizations of vector fields from an ensemble using an inverse projection technique. One approach is to project the original vector field ensemble in an $\mathbb{R}^2$ space using MDS and, for a given point $\mathbf{p}$, perform an inverse projection to generate a new realization. Another approach consists in, through the NHHD method, derive three ensembles for the rotational-free, divergence-free and harmonic components. After that, similarly to the first strategy, performing an inverse projection on points in these three projection spaces it is possible to obtain a new vector field realization. Here, we compared both RBF and Shepard's interpolation methods to perform the inverse projection step.

C. Radial Basis Interpolation

A *Radial Basis Function* (RBF) ϕ is a function whose value at $\mathbf{x}$ depends only on the distance from $\mathbf{x}$ to a certain point $\mathbf{p}$, i.e., $\phi(\mathbf{x}) = f(\|\mathbf{x} - \mathbf{p}\|)$ with $\| \cdot \|$ being often the Euclidean norm.

Recently, an inverse projection technique based on RBF interpolation was proposed [6], providing a smooth and global mapping from low to high dimensions. In RBF interpolation, for n data points $\mathbf{p_i} \in \mathbb{R}^2$ and their respective function values $q_i \in \mathbb{R}$, an interpolation function $s : \mathbb{R}^2 \to \mathbb{R}$ is computed in such a way that is possible to derive the value s for any arbitrary point in $\mathbf{p} \in \mathbb{R}^2$ according to the equation:

$$s(\mathbf{p}) = \sum_{i=1}^{n} \lambda_i \phi(\|\mathbf{p} - \mathbf{p}_i\|), \tag{2}$$

where λ_i, $i = 1, \ldots, n$, are the real-valued coefficients obtained by the interpolation method given the RBF kernel function ϕ. Such function s has to satisfy $s(\mathbf{p}_i) = q_i$, for $i = 1, \ldots, n$. Thus, to find the scalar coefficients λ_i, we have to solve the linear system $\Phi\Lambda = Q$, where Φ is the interpolation matrix with $\phi_{ij} = \phi_{ji} = \phi(\|\mathbf{p}_i - \mathbf{p}_j\|)$, $\Lambda = [\lambda_1 \cdots \lambda_n]^T$ and $Q = [q_1 \cdots q_n]^T$. In this work, we adopted the Gaussian kernel $\phi(r) = e^{-\varepsilon r^2}$, where ε is a positive parameter set to 1 and r is the Euclidean distance between a pair of points in $\mathbb{R}^2$. It is well known that the choice of ε affects the smoothness of the interpolation function $s(\mathbf{p})$.

Similar to Amorim et al. [6], this work aims to use an inverse projection technique of a point $\mathbf{p} \in \mathbb{R}^2$ to obtain a new 2D vector field realization. To do so, we have to build 2 (one for the $x-$ and the other for $y-$ coordinates) times $r \times c$ (the grid dimension) interpolation functions, or in other words: we have to solve $2 \times r \times c$ linear systems of equations. An efficient way to do that is to decompose the symmetric matrix Φ in the LU or in the LDLT form [26], and to solve the $2 \times r \times c$ linear systems of equations $\Phi\Lambda_l = B_l$ by the use of the forward and backward substitution methods. So, for the $x-$ and $y-$ coordinates and for each point $\mathbf{p}_i$ in the 2D grid we find the associated λ_i coefficients. Then, these can be used to derive the correspondent vector field for any arbitrary point $\mathbf{p} \in \mathbb{R}^2$ according to Equation 2.

D. Shepard's Interpolation

Inverse Distance Weighting (IDW) is a type of deterministic method for multivariate interpolation given a scattered set of points. Unknown points are derived through a weighted average of the values at the given ones. Shepard's Interpolation method [27] is a IDW originally proposed to produce a continuous surface from an irregularly-spaced one. To find the interpolated value f at a given point $\mathbf{p}$ based on known values $q_i = f(\mathbf{p}_i),\ i \in 1 \cdots n$ consists in calculating:

$$f(\mathbf{p}) = \begin{cases} \sum_{i=1}^{n} q_i \cdot w_i(\mathbf{p}), & \text{if } d_i(\mathbf{p}) \neq 0 \text{ for all } i \\ q_i, & \text{if } d_i(\mathbf{p}) = 0 \text{ for any } i \end{cases}, \quad (3)$$

where $d_i(\mathbf{p}) = \ \parallel \mathbf{x} - \mathbf{x}_i \parallel$, and $w_i(\mathbf{x}) = \frac{1/d_i(\mathbf{x})^l}{\sum_{j=1}^{n} 1/d_i(\mathbf{x})^l}$.

Given that, the weights w increase accordingly to the distance of $\mathbf{p}$ to the known points, where greater values means greater influence of a given point. The parameter l controls the influence of the input points. In this work, we set l to 2.

Opposite to Amorim et al. approach [6], Shepard's Interpolation doesn't require solving any linear system of equations. Notwithstanding, for each given point $\mathbf{p}$ in the projection space, it is necessary to calculate once the weight values $w_i = \ \ i \in 1, \ldots, n$ to be used in Equation 3. In this work, we apply the formula in Equation 3 to the vector coordinate at each point in $\mathbb{S}_{r,c} = \{\mathbf{x}_{i,j} \in \mathbb{R}^2 : 1 \leq i \leq r, 1 \leq j \leq c\}$. In other words, we use two interpolation functions, one for each coordinate.

V. Generating Vector Field Realizations

As described above, we propose two ways to interactively generate a new vector field realization from an ensemble. The first one is accomplished based on the original vector field ensemble. The second one is made through the combination of the HHD components of the original data set. In both cases, the first step consists in performing a multidimensional reduction, through MDS, transforming the vector field data from $\mathbb{R}^{2\times r\times c}$ to $\mathbb{R}^2$. Doing that, we can provide a visualization of those data allowing an user to generate a new realization exploring a low dimensional space, i.e., a new vector field can be generated for any given point in the screen.

For the first case, when a point is selected in the projection space (Figure 1), its inverse projection is obtained according to the techniques presented in the previous section. For the second case, three points – one for each of the HHD components – are required to generate a new realization (Figure 2). Here, a new realization is obtained as the sum of the inverse projection of each one of the given points, as stated by the Helmholtz-Hodge Decomposition.

Using the `Ctrl` key, a selected point is bonded to the closest projected point. This means that, for the HHD-based vector field generation, an original component can be used.

VI. Results and Discussion

To test the proposed approach, we make use of a 2D vector field ensemble comprehended by eight multi-method wind forecast realizations ξ, provided by the Brazilian Instituto Nacional de Pesquisas Espaciais (INPE). These realizations are delimited, in polar coordinates, by $-47°, 11.0195°$ and $277.867°, 333.097°$ as the latitude and longitude coordinates

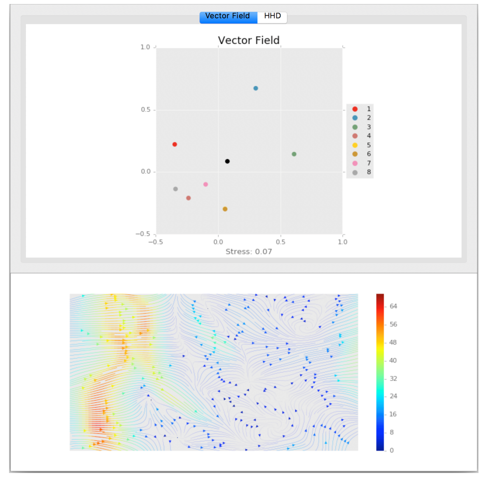

Fig. 1: A black marker in the MDS plot represents the chosen point to be used in the inverse projection. The bottom plot shows the resulting vector field.

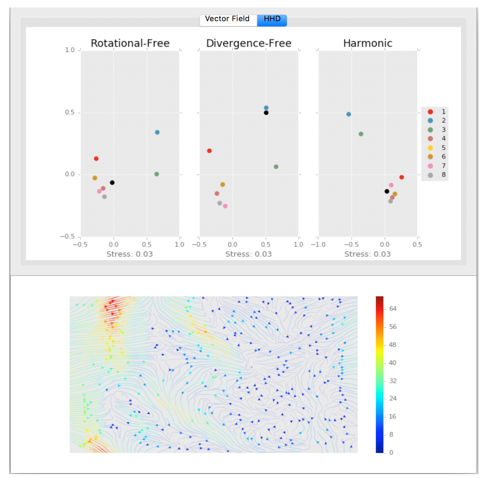

Fig. 2: Generating a realization from the HHD components requires a point to be selected for the rotational-free, divergence-free and harmonic components projection spaces.

range, in that order. This region is defined over a Cartesian grid structure of 72×82 cells. Figure 3 presents the mean vector field for this data set, as well as for its rotational-free, divergence-free and harmonic components, in that order. Their multidimensional projection can be found in Figures 1 and 2.

A. Quality Assessment

To verify the quality of the results obtained with the proposed method, we performed two tests. Firstly, we would like to check the hypothesis that the HHD inversion technique approach is capable of providing higher variability than deriving new realizations from the original data ensemble, which we will state as the *standard* approach. To do so, we generated 100 scenarios using the HHD technique and 100 other ones through the latter. For each one of these two sets (from now on we will call them $\mathcal{E}_{VF}$ and $\mathcal{E}_{HHD}$, respectively) we calculated the curl and divergence operators, as well as the norm, and

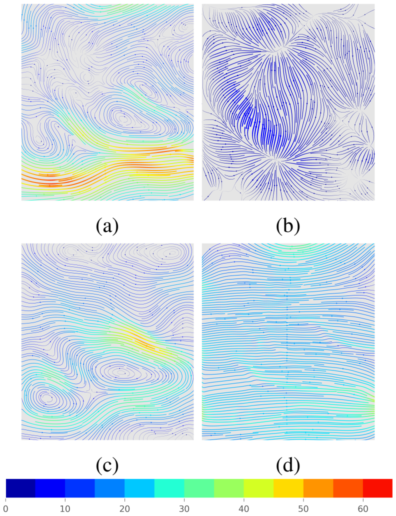

Fig. 3: Mean vector field for the the multi-method wind forecast realizations (a) and its HHD components (rotational-free – (c), divergence-free – (e), and harmonic – (g), respectively). The color map represents the vector field magnitude and its common for all realizations, original or derived.

computed their variability. Secondly, we randomly chose some of the generated scenarios, for both approaches, to qualitatively analyze their similarity with the input ensemble.

From the first test we have got to the following conclusions:

a) RBF Interpolation: The HHD approach provides higher variability than the standard approach. However, it generates a wider number of outliers. Moreover, in some cases the RBF Interpolation can lead to extreme scenarios, inconsistent with the input data ensemble.

b) Shepard's Interpolation: To overcome the problem faced when using the RBF Interpolation method, we chose to apply the Shepard's Interpolation technique to generate new scenarios given a set of projected points. We chose this interpolation method due to the higher control of the outcomes that it can provide. Whilst it leads to a lower variability of scenarios when compared to the RBF (Figure 4), no extreme scenarios were observed.

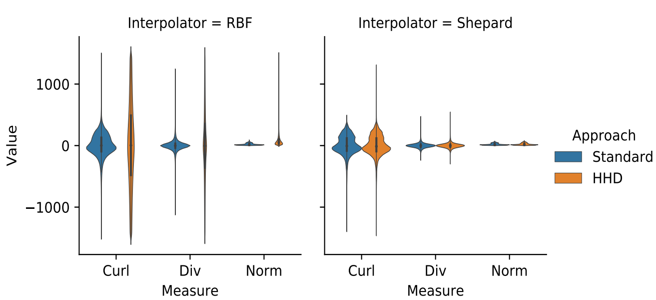

Fig. 4: Distribution of the curl, divergence and norm for the scenarios generated using the proposed approaches.

For the second test, Tables I and II present some of the realizations obtained using both interpolation techniques, for the standard and HHD approaches, respectively. One can see that the RBF Interpolation can lead to inconsistent outputs, in which both the norm and the vector field's direction present discontinuities. In opposition, the Shepard's Interpolation provide smooth outputs. However, they are more similar among themselves, i.e., they lead to a lower variability when compared to the latter method. Notwithstanding, as this variability is similar to the original ensemble one, we believe that this interpolation is capable of generating a good range of different scenarios.

VII. Conclusion

In this work, we proposed the application of dimensional reduction and inverse projection to generate 2D vector fields given an ensemble. Through the Helmholtz-Hodge Decomposition we presented an approach to increase the range of the possible outcomes. More than that, through this technique the maintenance of specific features can be achieved. We also compared the use of the RBF Interpolation with the Shepard's Interpolation. Results show that, in both cases, the Helmholtz-Hodge approach is capable of increase the variability of the possible generated vector fields. Notwithstanding, we could verify that the RBF Interpolation generated extreme scenarios, where the norm of the vector fields, as well as the curl and divergence operators, presented a huge amount of variability in comparison with the input ensemble, which means that this approach lead to inconsistent and unstable scenarios. On the other hand, using the Shepard's Interpolation we were able to achieve better results, since this method provides more control of the possible outputs. However, as a drawback the obtained variability was a bit smaller than the input ensemble's one. In general, this approach was capable of generating realizations with some variability whilst respecting the given ones.

For the future, we plan to evaluate the achieved results with expertises in applications that make use of this kind of data, to access the validity of the scenarios application-based. We also would like to test the presented approach with a multidimensional projection that uses control points, as the LAMP [10], for example. Besides, we plan to apply this technique with 3D vector fields, as well as to expand this study to other types of multivariate data.

Acknowledgments

We would like to thank CNPq and PETROBRAS for partially supporting this research. Additionally, we would like to thank **INPE**, Alex Almeida Fernandes and Haroldo Fraga de Campos Velho for the wind forecast data models used in this work.

References

[1] M. Beccali, M. Cellura, and M. Mistretta, "Decision-making in energy planning. application of the electre method at regional level for the diffusion of renewable energy technology," *Renewable Energy*, vol. 28, no. 13, pp. 2063–2087, 2003.

[2] G. Mariethoz and J. Caers, *Multiple-point geostatistics: stochastic modeling with training images*. John Wiley & Sons, 2014.

[3] J. D. Anderson and J. Wendt, *Computational fluid dynamics*. Springer, 1995, vol. 206.

TABLE I: Samples of the obtained realizations for the RBF and Shepard's Interpolations, for the standard approach. The points $(\cdot, \cdot)$ used for the inverse projection are listed on the top.

$(0.2, 0.2)$	$(0.61890625, 0.725)$	$(0.78765625, -0.35625)$	$(-0.36234375, 0.86875)$
RBF Interpolation			
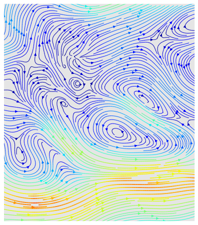	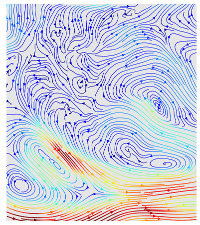	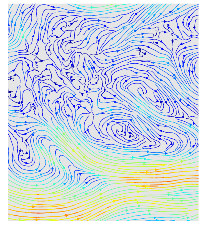	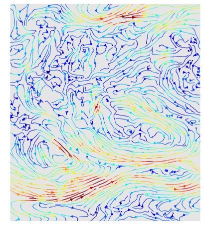
Shepard's Interpolation			
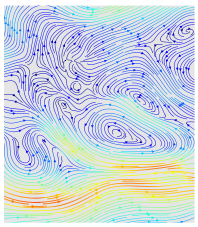	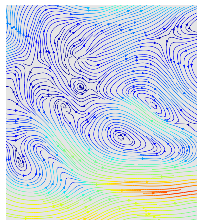	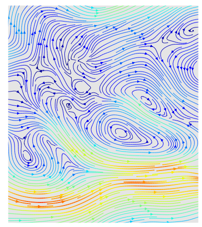	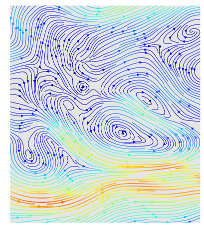

[4] Y. Tong, S. Lombeyda, A. N. Hirani, and M. Desbrun, "Discrete multiscale vector field decomposition," *ACM Trans. Graph.*, vol. 22, no. 3, pp. 445–452, Jul. 2003.

[5] C. Luo, I. Safa, and Y. Wang, "Feature-aware streamline generation of planar vector fields via topological methods," *Computers & Graphics*, vol. 36, no. 6, pp. 754–766, 2012. [Online]. Available: http://dx.doi.org/10.1016/j.cag.2012.04.014

[6] E. Amorim, E. Vital Brazil, J. Mena-Chalco, L. Velho, L. G. Nonato, F. Samavati, and M. Costa Sousa, "Facing the high-dimensions: Inverse projection with radial basis functions," *Computer & Graphics*, vol. 48, no. C, pp. 35–47, May 2015. [Online]. Available: http://dx.doi.org/10.1016/j.cag.2015.02.009

[7] I. Jolliffe, *Principal Component Analysis*. Springer Verlag, 1986.

[8] T. F. Cox and M. Cox, *Multidimensional Scaling, Second Edition*, 2nd ed. Chapman and Hall/CRC, 2000.

[9] L. van der Maaten and G. Hinton, "Visualizing High-Dimensional Data Using t-SNE," *Journal of Machine Learning Research*, vol. 9, pp. 2579–2605, Nov. 2008.

[10] P. Joia, D. B. Coimbra, J. A. Cuminato, F. V. Paulovich, and L. G. Nonato, "Local affine multidimensional projection," *IEEE Transactions on Visualization and Computer Graphics*, vol. 17, no. 12, pp. 2563–2571, 2011. [Online]. Available: http://dx.doi.org/10.1109/TVCG.2011.220

[11] A. J. Chorin and J. E. Marsden, *A mathematical introduction to fluid mechanics*, 3rd ed., ser. Texts in Applied Mathematics. Springer-Verlag, 1993.

[12] E. P. dos Santos Amorim, E. V. Brazil, J. D. II, P. Joia, L. G. Nonato, and M. C. Sousa, "ilamp: Exploring high-dimensional spacing through backward multidimensional projection." in *IEEE VAST*. IEEE Computer Society, 2012, pp. 53–62. [Online]. Available: http://doi.ieeecomputersociety.org/10.1109/VAST.2012.6400489

[13] W. Casaca, E. G. Nieto, C. O. L. Ferreira, G. Tavares, P. A. Pagliosa, F. V. Paulovich, L. G. Nonato, and A. Paiva, "Colorization by multidimensional projection," in *25th SIBGRAPI Conference on Graphics, Patterns and Images*, 2012, pp. 32–38. [Online]. Available: http://dx.doi.org/10.1109/SIBGRAPI.2012.14

[14] R. M. Martins, G. F. Andery, H. Heberle, F. V. Paulovich, A. de Andrade Lopes, H. Pedrini, and R. Minghim, "Multidimensional projections for visual analysis of social networks," *Journal of Computer Science and Technology*, vol. 27, no. 4, pp. 791–810, 2012. [Online]. Available: http://dx.doi.org/10.1007/s11390-012-1265-5

[15] K. Kim and J. Lee, "Sentiment visualization and classification via semi-supervised nonlinear dimensionality reduction," *Pattern Recogn.*, vol. 47, no. 2, pp. 758–768, Feb. 2014. [Online]. Available: http://dx.doi.org/10.1016/j.patcog.2013.07.022

[16] F. Schroff, D. Kalenichenko, and J. Philbin, "Facenet: A unified embedding for face recognition and clustering," in *The IEEE Conference on Computer Vision and Pattern Recognition (CVPR)*, June 2015.

[17] J. C. Gomez and M.-F. Moens, "PCA document reconstruction for email classification," *Computational Statistics & Data Analysis*, vol. 56, no. 3, pp. 741 – 751, 2012. [Online]. Available: http://dx.doi.org/10.1016/j.csda.2011.09.023

[18] G. M. H. Mamani, F. M. Fatore, L. G. Nonato, and F. V. Paulovich, "User-driven feature space transformation," *Comput. Graph. Forum*, vol. 32, no. 3, pp. 291–299, 2013. [Online]. Available: http://dx.doi.org/10.1111/cgf.12116

[19] D. Motta, W. Casaca, P. Pagliosa, and A. Paiva, "A user-friendly interactive framework for unsteady fluid flow segmentation and visualization," *Journal of Visualization*, pp. 1–12, 2018.

[20] H. Bhatia, G. Norgard, V. Pascucci, and P. Bremer, "The Helmholtz-Hodge Decomposition - A Survey," *IEEE Transactions on Visualization and Computer Graphics*, vol. 19, no. 8, pp. 1386–1404, 2013.

[21] H. Wang and J. Deng, "Feature extraction of complex ocean flow field using the helmholtz-hodge decomposition," in *2013 IEEE International Conference on Multimedia and Expo Workshops*. IEEE, 2014, pp. 1–6.

[22] H. Gao, M. K. Mandal, G. Guo, and J. Wan, "Singular point detection using discrete hodge helmholtz decomposition in fingerprint images." in *ICASSP'10*. IEEE, 2010, pp. 1094–1097.

[23] P. C. Ribeiro, H. F. de Campos Velho, and H. Lopes, "Helmholtz-hodge decomposition and the analysis of 2d vector field ensembles," *Computers & Graphics*, vol. 55, pp. 80–96, 2016. [Online]. Available: http://dx.doi.org/10.1016/j.cag.2016.01.001

[24] V. Pascucci, P.-T. Bremer, and H. Bhatia, "The Natural Helmholtz-Hodge Decomposition For Open-Boundary Flow Analysis," *IEEE Transactions on Visualization and Computer Graphics*, vol. 99, no. PrePrints, pp. 1–11, 2014.

[25] J. B. Kruskal, "Multidimensional scaling by optimizing goodness of fit to a nonmetric hypothesis," *Psychometrika*, vol. 29, no. 1, pp. 1–27, 1964. [Online]. Available: http://dx.doi.org/10.1007/BF02289565

[26] G. H. Golub and C. F. Van Loan, *Matrix computations*. JHU Press, 2012, vol. 3.

[27] D. Shepard, "A two-dimensional interpolation function for irregularly-spaced data," in *Proceedings of the 1968 23rd ACM National Conference*, ser. ACM '68. New York, NY, USA: ACM, 1968, pp. 517–524. [Online]. Available: http://doi.acm.org/10.1145/800186.810616

TABLE II: Samples of the obtained realizations for the RBF and Shepard's Interpolations, for the HHD approach. The points $(\cdot,\cdot)$ used for the inverse projection are listed on the top.

	Rotational-Free	Divergence-Free	Harmonic	Vector Field
	$(-0.0170371, 0.05)$	$(-0.02632535, 0.075)$	$(-0.14747903, 0.0375)$	
RBF Interpolation	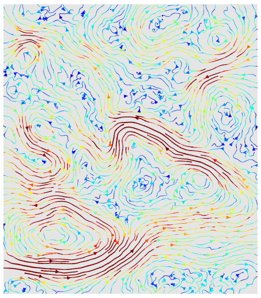	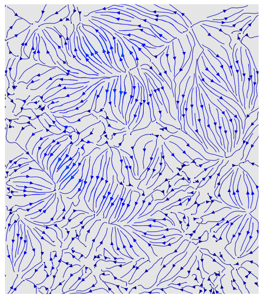	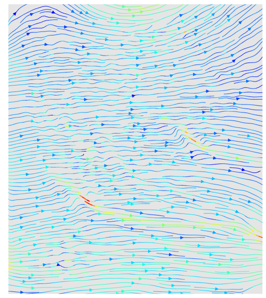	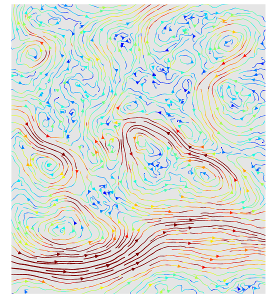
Shepard's Interpolation	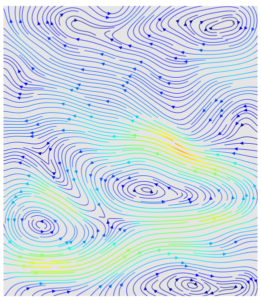	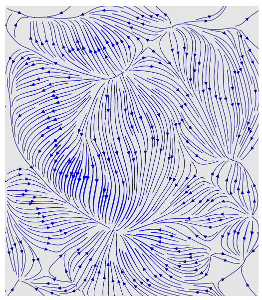	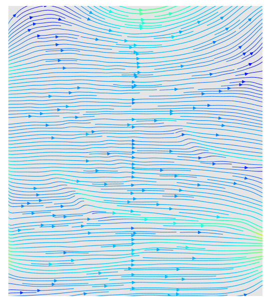	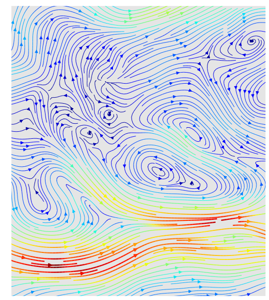
	$(0.65337715, 0.24375)$	$(0.5117703, -0.01875)$	$(-0.00633919, 0.475)$	
RBF Interpolation	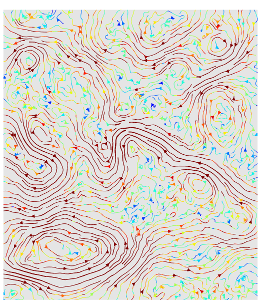	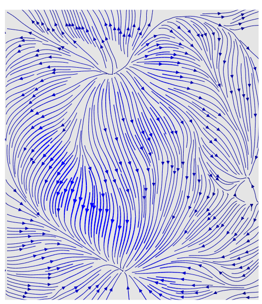	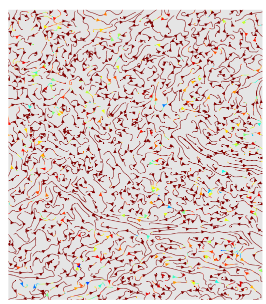	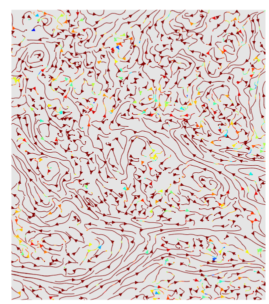
Shepard's Interpolation	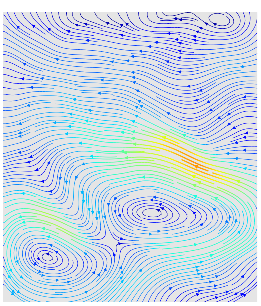	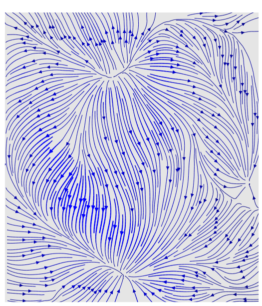	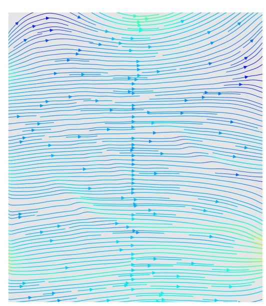	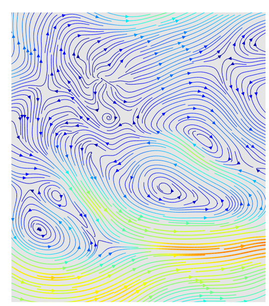

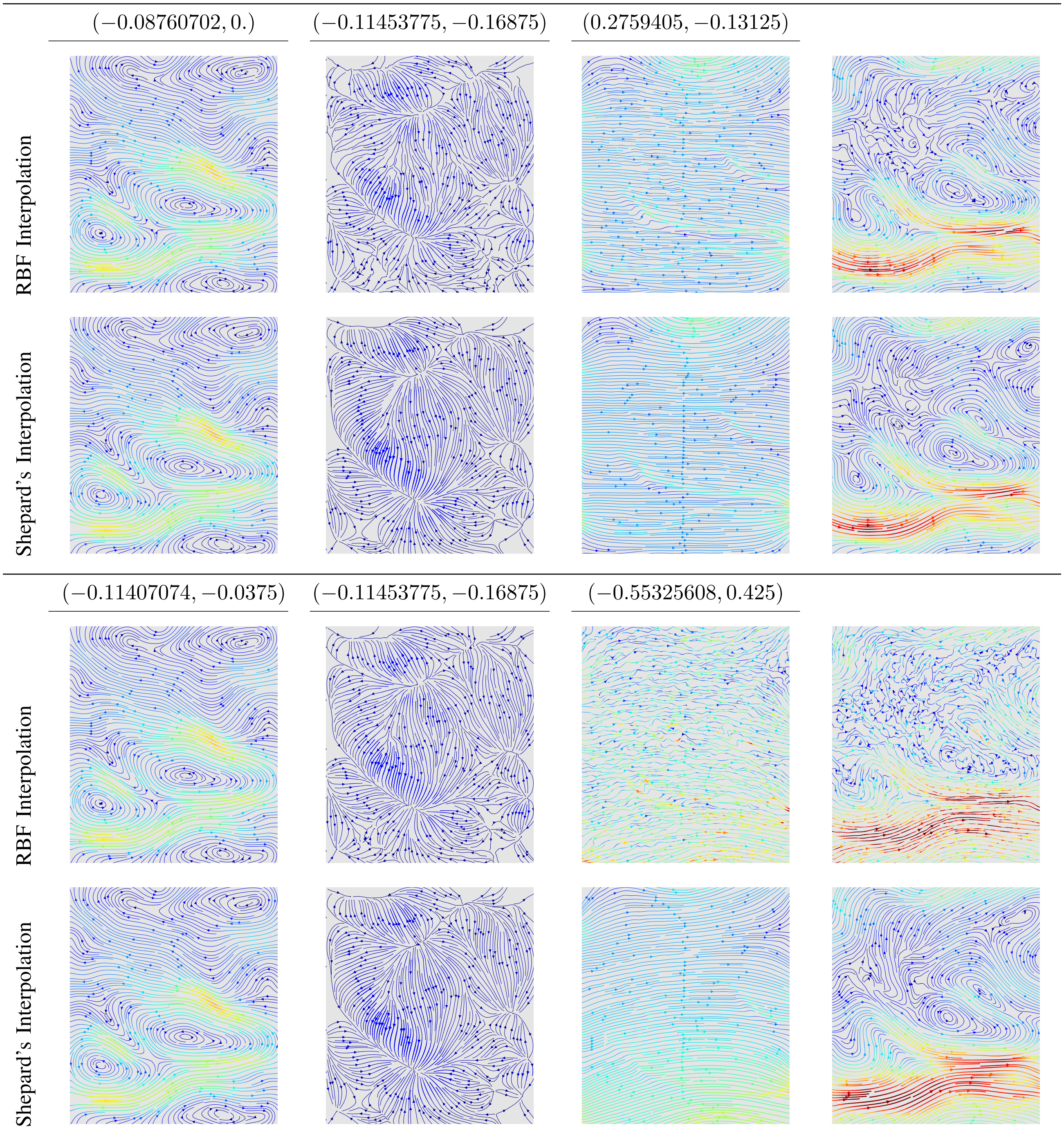
(−0.08760702, 0.)
(−0.11453775, −0.16875)
(0.2759405, −0.13125)
RBF Interpolation
Shepard's Interpolation
(−0.11407074, −0.0375)
(−0.11453775, −0.16875)
(−0.55325608, 0.425)
RBF Interpolation
Shepard's Interpolation